Mesoporous Silica Fibers: Synthesis, Internal Structure, and Growth Kinetics

Freddy Kleitz,[†] Frank Marlow,*[,†] Galen D. Stucky,[‡] and Ferdi Schüth[†]

Max-Planck-Institut für Kohlenforschung, 45470 Mülheim an der Ruhr, Germany, and Department of Chemistry and Biochemistry, University of California, Santa Barbara, California 93106-9510

Received February 5, 2001. Revised Manuscript Received August 9, 2001

The influence of the silica source on the morphology and the internal architecture of mesoporous fibers was investigated. It was found in all cases studied that the hexagonally packed pores are oriented in a circular manner around the fiber axis. However, the kinetics of fiber formation and the product distribution vary, being strongly dependent on the silica source and the amount of an additional oil. Electron microscopy and XRD investigations were carried out to elucidate the morphological and structural features of the mesoporous silica materials. The properties of the materials on the nanometer and micrometer scale are shown to depend on the silica precursor hydrolysis rate and micelle swelling effects. The experiments also revealed that gravity plays no essential role in the growth of the fibers.

Introduction

Mesoporous materials of the MCM-41,[1] FSM,[2] and SBA-type[3] families have been widely studied with respect to their structure and morphology, which have been reviewed several times recently.[4] The nature of the inorganic precursors and the variations in the synthesis conditions are crucial factors for the efficient design of materials with desired architectures. Recently, much work has focused on developing new classes of inorganic materials with hierarchical structure and well-defined macroscopic forms. Mesoporous thin films,[5−12] spheres,[13,14] curved-shaped solids,[15] tubes,[16,17] rods,[18] fibers,[19−22] membranes,[23] and other monoliths[24,25] were prepared. To achieve this, simultaneous control of the structural parameters on the nanometer scale and the morphology on the micrometer scale are required. This can be of particular interest for optical devices,[26−28] for which the organization of the materials on different length scales is decisive.

As described in a previous paper,[28] dye-doped mesoporous fibers present such an organization, owing to the

* To whom correspondence should be addressed. E-mail: marlow@mpi-muelheim.mpg.de.

[†] Max-Planck-Institut für Kohlenforschung.

[‡] University of California.

(1) (a) Kresge, C. T.; Leonowicz, M. E.; Roth, W. J.; Vartuli, J. C.; Beck, J. S. *Nature* **1992**, *359*, 710−712. (b) Beck, J. S.; Vartuli, J. C.; Roth, W. J.; Leonowicz, M. E.; Kresge, C. T.; Schmitt, K. D.; Chu, C. T.-W.; Olson, D. H.; Sheppard, E. W.; McCullen, S. B.; Higgins, J. B.; Schlenker, J. L. *J. Am. Chem. Soc.* **1992**, *114*, 10834−10843.

(2) (a) Yanagisawa, T.; Shimizu, T.; Kuroda, K.; Kato, C. *Bull. Chem. Soc. Jpn.* **1990**, *63*, 988−992. (b) Inagaki, S.; Koiwai, A.; Suzuki, N.; Fukushima, Y.; Kuroda, K. *Bull. Chem. Soc. Jpn.* **1996**, *69*, 1449−1457.

(3) (a) Huo, Q.; Margolese, D. I.; Ciesla, U.; Feng, P.; Gier, T. E.; Sieger, P.; Leon, R.; Petroff, P. M.; Schüth, F.; Stucky, G. D. *Nature* **1994**, *368*, 317−321. (b) Huo, Q.; Margolese, D. I.; Ciesla, U.; Demuth, D. G.; Feng, P.; Gier, T. E.; Sieger, P.; Firouzi, A.; Chmelka, B. F.; Schüth F.; Stucky, G. D. *Chem. Mater.* **1994**, *6*, 1176−1160. (c) Huo, Q.; Leon, R.; Petroff, P. M.; Stucky, G. D. *Science* **1995**, *268*, 1324−1327. (d) Huo, Q.; Margolese, D. I.; Stucky, G. D. *Chem. Mater.* **1996**, *8*, 1147−1160. (e) Zhao, D.; Feng, J.; Huo, Q.; Melosh, N.; Fredrickson, G. H.; Chmelka, B. F.; Stucky, G. D. *Science* **1998**, *279*, 548−552.

(4) (a) Lindén, M.; Schacht, S.; Schüth, F.; Steel, A.; Unger, K. K. *J. Porous Mater.* **1998**, *5*, 177−193. (b) Ciesla, U.; Schüth, F. *Microporous Mesoporous Mater.* **1999**, *27*, 131−149. (c) Ozin, G. A. *Chem. Commun.* **2000**, 419−432.

(5) Yang, H.; Kuperman, A.; Coombs, N.; Mamiche-Afara, S.; Ozin, G. A. *Nature* **1996**, *379*, 703−705.

(6) Yang, H.; Coombs, N.; Sokolov, I.; Ozin, G. A. *Nature* **1996**, *381*, 589−592.

(7) Lu, Y.; Ganguli, R.; Drewien, C. A.; Anderson, M. T.; Brinker, C. J.; Gong, W.; Guo, Y.; Soyez, H.; Dunn, B.; Huang, M. H.; Zink, J. I. *Nature* **1997**, *389*, 364−368.

(8) Ryoo, R.; Ko, C. H.; Cho, S. J.; Kim, J. M. *J. Phys. Chem. B* **1997**, *101*, 10610−10613.

(9) Hillhouse, H.; Okubo, T.; van Egmond, J. W.; Tsapatsis, M. *Chem. Mater.* **1997**, *9*, 1505−1507.

(10) Zhao, D.; Yang, P.; Melosh, N.; Feng, J.; Chmelka, B. F.; Stucky, G. D. *Adv. Mater.* **1998**, *10*, 1380−1385.

(11) Miyata, H.; Kuroda, K. *Chem. Mater.* **1999**, *11*, 1609−1614.

(12) Ogawa, M.; Masukawa, N. *Microporous Mesoporous Mater.* **2000**, *38*, 35−41.

(13) Schacht, S.; Huo, Q.; Voigt-Martin, I. G.; Stucky, G. D.; Schüth, F. *Science* **1996**, *273*, 768−771.

(14) Grün, M.; Lauer, I.; Unger, K. K. *Adv. Mater.* **1997**, *9*, 254−257.

(15) Ozin, G. A; Yang, H.; Sokolov, I.; Coombs, N. *Adv. Mater.* **1997**, *9*, 662−667.

(16) Lin, H.-P.; Mou, C.-Y. *Science* **1996**, *273*, 765−768.

(17) Lin, H.-P.; Cheng, S.; Mou, C.-Y. *Chem. Mater.* **1998**, *10*, 581−589.

(18) Schmidt-Winkel, P.; Yang. P.; Margolese, D. I.; Chmelka, B. F.; Stucky, G. D. *Adv. Mater.* **1999**, *11*, 303−307.

(19) Bruinsma, P. J.; Kim, A. Y.; Liu, J.; Baskaran, S. *Chem. Mater.* **1997**, *9*, 2507−2512.

(20) Lin, H.-P.; Mou, C.-Y.; Liu, S.-B. *Adv. Mater.* **2000**, *12*, 103−106.

(21) Yang. P.; Zhao, D.; Chmelka, B. F.; Stucky, G. D. *Chem. Mater.* **1998**, *10*, 2033−2036.

(22) Miyata, H.; Kuroda, K. *Adv. Mater.* **2001**, *13*, 558−561.

(23) Zhao, D.; Yang, P.; Chmelka, B. F.; Stucky, G. D. *Chem. Mater.* **1999**, *11*, 1174−1178.

(24) Göltner, C. G.; Henke, S.; Weissenberger, M. C.; Antonietti, M. *Angew. Chem., Int. Ed. Engl.* **1998**, *37*, 613−616.

(25) Melosh, N. A.; Davidson, P.; Chmelka, B. F. *J. Am. Chem. Soc.* **2000**, *22*, 823−829.

(26) Lebeau, B.; Fowler, C. E.; Hall, S. R.; Mann, S. *J. Mater. Chem.* **1999**, *9*, 2279−2281.

(27) Wirnsberger, G.; Stucky, G. D. *Chem. Mater.* **2000**, *12*, 2525−2527.

(28) Marlow, F.; McGehee, M. D.; Zhao, D.; Chmelka, B. F.; Stucky, G. D. *Adv. Mater.* **1999**, *11*, 632−636.

10.1021/cm0110324 CCC: $20.00
Published on Web 09/26/2001

presence of a molecular dye within the hexagonally ordered mesophase and the homogeneous cylindrical morphology of the fibers. Therefore, they could be used as high surface area optical waveguides[29] or as a new type of laser material.[28]

The spontaneous growth of high-quality, hexagonal phase mesoporous silica fibers was originally reported in 1997.[29] The fibers were obtained from a static two-phase acidic system, allowing a slow growth of the silica mesophase. At this time it was stated that the fibers consist of hexagonally organized channels oriented parallel to the fiber axis, as is suggested for SBA-15-based fibers[21,30] and other fibers.[19,22] However, further investigations suggested that this hypothesis could be incorrect. Fibers synthesized with tetrabutoxysilane in absence of additional oil were shown to have a circular inner architecture, consisting of hexagonally organized channels running circularly around the fibers axis.[31,32]

The acidic fiber synthesis is highly flexible. It is possible to use various silicon sources, surfactants, and additional oils. Moreover, the temperature, the pH, and the solution ionic strength have an influence on the growth of the solids. Different morphologies and shapes can be obtained. Fibers with various thickness, length, and surface roughness have been found, but the precise function of all the parameters mentioned is still unclear. Up to now, it is also an open question whether all the mesoporous silica fibers obtained from a two-phase acidic system have the same circular internal pore arrangement that has been evidenced for the TBOS-based synthesis. Since changes in silica source and the addition of oil are expected to affect the kinetics of the reaction and the nucleation process, the materials obtained could present diverse hierarchical structures.

The aim of the present work is to investigate whether the circular structure is observed for a larger range of synthesis conditions. Therefore, we have systematically changed the nature of the silicon alkoxides and the type of organics used as additional oil. We show that the fibers obtained from acidic syntheses using either TEOS or TPOS in various oils, which change the reaction rates over orders of magnitude, always have the same characteristics with the channels whirling around the center of the fiber. Therefore, we can now regard the circular internal structure as a general property of mesostructured fibers obtained in static system under acidic conditions. This corrects previous statements concerning the fibers architecture.

Experimental Section

Synthesis. The synthesis of the fibers was based on the procedure described previously.[28] The molar composition of the initial aqueous synthesis mixture was 100 H_2O:0.0246 alkyltrimethylammonium halide:2.92 HCl, which was prepared with stirring. $CH_3(CH_2)_{15}N(CH_3)_3Br$ (CTAB), $CH_3(CH_2)_{13}N(CH_3)_3$-Br (C14TAB), or $CH_3(CH_2)_{15}N(CH_3)_3Cl$ (CTAC) was used as cationic surfactant. Typically, 0.375 mmol of a silicon source reagent was added to 15 g of the aqueous surfactant solution in a closed 20 mL glass vessel without stirring. The syntheses were performed at room temperature.

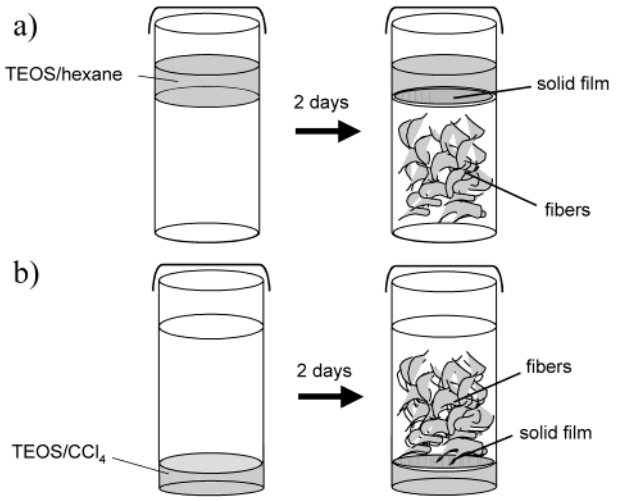

Figure 1. Schematic representation of the synthesis for static two-phase acidic systems. (a) TEOS in hexane, (b) TEOS in CCl_4.

Different silicon alkoxides were studied as silica precursors. If additional oil was used, the silicon source was dissolved in the oil before the addition to the aqueous solution. We used $(C_4H_9O)_4Si$ (TBOS) without any additional oil, and the spontaneous growth of the fibers was typically observed in the water phase after 2 days. $(C_2H_5O)_4Si$ (TEOS) was mixed with either *n*-hexane, CCl_4, mesitylene, or toluene. The same amount of TEOS (0.375 mmol) was dissolved in 3.75, 1.5, 0.750, and 0.375 mL of oil. The mixture was then added to the aqueous solution and left under quiescent conditions. In the case of CCl_4, the aqueous solution was added dropwise to the silicon precursor solution, since here the aqueous phase is at the top. In all syntheses, spontaneous growth of fibers was observed in the water phase within 24 h. A solid thin layer forms at the interface between the two phases (Figure 1). In the present work, we will refer to it as "solid film". The fibers obtained from the TEOS-based systems were removed from the synthesis batch after 7 days and dried at room temperature for 4 days.

Alternatively, $(C_3H_7O)_4Si$ (TPOS) (0.375 mmol), either without or in *n*-hexane (0.375, 0.75, 1.5 mL) or in CCl_4 (0.075, 0.375, 0.75, 1.5 mL), was used as silica precursor. Generally, solid products were observed in the aqueous phase and at the interface within times ranging from 3 days to several weeks. The fibers obtained from a TPOS/hexane mixture were usually removed after 15 days and dried at room temperature for 4 days. In the case of CCl_4, the fibers were removed after 6 weeks.

Template-free samples were obtained by calcination in a box furnace in air at 500 °C for 8 h. The XRD measurements and nitrogen adsorption data are in agreement with the previous works.[29]

X-ray Powder Diffraction. The samples were analyzed with a STOE STADI P diffractometer equipped with a linear position-sensitive detector in transmission geometry using Cu $K\alpha_1$ radiation and allowing to measure 2θ angles down to 1.0°. XRD patterns were recorded in 2θ ranges of 1−7° with step of 0.01° and time per step of 1560 s.

Samples obtained from the TPOS/CCl_4 system were additionally analyzed on a GADDS diffractometer (Bruker axs) using Cu $K\alpha_1$ radiation in transmission geometry. The setup (Göbel mirrors, HI-STAR area detector, collimator aperture 0.8 mm, measurement time 600 s) allowed to measure 2θ angles down to 0.5°.

Scanning Electron Microscopy. A Hitachi S-3500N scanning electron microscope was used. The microscope was operated at 5 or 25 keV. The samples were coated by a 10 nm layer of gold.

(29) Huo, Q.; Zhao, D.; Feng, J.; Weston, K.; Buratto, S. K.; Stucky, G. D.; Schacht, S.; Schüth, F. *Adv. Mater.* **1997**, *9*, 974−978.
(30) Han, Y.-J.; Kim, J. M.; Stucky, G. D. *Chem. Mater.* **2000**, *12*, 2068−2069.
(31) Marlow, F.; Spliethoff, B.; Tesche, B.; Zhao, D. *Adv. Mater.* **2000**, *12*, 961−965.
(32) Marlow, F.; Zhao, D.; Stucky, G. D. *Microporous Mesoporous Mater.* **2000**, *39*, 37−42.

Transmission Electron Microscopy. A Hitachi HF 2000 transmission electron microscope operated at 200 keV was used which was equipped with a cold field emission source. Calcined samples have been used which were mounted on carbon films which were fixed on copper grids.

Product Statistics. The percentage of fibers and small particles in the sample were estimated statistically from overview SEM pictures. A grid (16 columns × 12 lines) was overlaid on each representative SEM micrograph, and the shape of the each solid particle observed at the grid line intersections was registered.

Kinetics Studies. The solid products form a stable layer in the solution with a thickness which can be directly measured with a ruler. Alternatively, the mass of solid products has been determined. For this, a synthesis batch was filtered and rinsed with 10 mL of heptane. After this, the filter paper together with the solid products was calcined. The product consists of SiO_2 which was weighted. The main reason for the scatter of data points results from the use of different batches which have slightly different growth kinetics. The thickness measurements do not disturb the synthesis and can be applied for one single batch.

Results

Synthesis Products. Synthesis studies have been carried out with tetraethoxysilane (TEOS), tetrapropoxysilane (TPOS), and tetrabutoxysilane (TBOS) as silica sources in the presence of hexane and CCl_4. These systems separate into two phases as schematically shown in Figure 1. The presence of oil allows the growth of fibers in systems with silicon sources such as TEOS, which hydrolyze quickly in an aqueous environment. The more slowly reacting TBOS forms fibers without additional oil. As intermediate situation, pure TPOS and diluted with different oils have been investigated as well.

In all systems studied, the fiber growth starts in the region close to the interface of the aqueous and organic phases. Depending on the conditions, highly transparent fibers with thicknesses ranging from submicrons to 40 μm were obtained in the aqueous phase, within times ranging from some hours to several weeks. Examples of the products collected from various systems are shown in Figure 2. Generally, one can observe among the synthesis products different proportions of long homogeneous fibers, shorter fibers with variable thickness, flat elongated solids, and small circular particles. Fibers with a length ranging from a few microns up to several millimeters can be found. We note that the syntheses performed in the presence of CCl_4 produce very similar products. As this oil has a higher density than water, these experiments make a decisive role of gravity in the fiber growth mechanism very unlikely (Figure 1).

The formation of hollow fibers is also possible. Examples of hollow fibers are shown in Figure 3. In the syntheses described in the present work, only small fractions of hollow solids were formed. The highest proportions of hollow fibers were observed in syntheses based on dilute TEOS with either hexane or CCl_4.

Depending on the amount and the nature of oil, the ratio of fibers toward other morphologies varies (Table 1). A general trend is that the syntheses with additional oil lead to thin fibers and a relatively high content of small circular particles (sometimes called gyroids). A solid film at the phase boundary was always observed. The average fiber thickness was found to be in the range from 2 to 10 μm for TEOS in hexane and from 1 to 6 μm for TEOS in CCl_4. The fiber synthesis carried out with pure TEOS as precursor leads to a very low total yield of mesostructured products (most of the silica formed is amorphous), with 50% of the mesostructured products consisting of fibers. By adding hexane to TEOS, the proportion of long homogeneous fibers increases as already observed in previous reports.[29] In a sample where only 0.375 mL of hexane was added to TEOS (Figure 2a), about 55% of the product is composed of fibers, whereas in a sample with 3.75 mL of hexane (Figure 2b), the amount of fibers increases to about 80%.

Also, CCl_4 as oil allows the synthesis of fibers. However, the dependence of the fiber fraction on the oil content was found to be opposite (see Table 1). The percentage of fibers in the samples where only 0.375 mL of CCl_4 was added is about 80% (Figure 2c). This percentage drops down to about 45% with addition of 3.75 mL of CCl_4 (Figure 2d). In addition, the products with CCl_4 as oil showed separated regions containing large quantities of small particles mixed with other domains containing primarily fibers.

In the case of TPOS, the quantity of fibers collected increases with the concentration of the silica source. Scanning electron micrographs of fibers obtained from TPOS in hexane and CCl_4 are shown in Figure 2e−h. Here, only very concentrated TPOS or pure TPOS lead to the formation of long homogeneous silica fibers. At high oil contents, small circular particles are predominantly formed. The average fiber thickness ranges from 5 up to 40 μm for syntheses using hexane or pure TPOS; the fibers obtained with the TPOS/CCl_4 silicon source show diameters between 2 and 10 μm.

Growth Kinetics. The addition of CCl_4 to TEOS leads to an interesting system with respect to the arrangement of the phases, and it is also very suitable for kinetic analysis since one can easily observe various stages of the fiber growth directly by eye. Figure 4 describes the macroscopic evolution of the TEOS in CCl_4 system which is very similar also for the other systems. In all cases, an induction period occurs before a visible layer of solid products is formed. The more concentrated the silicon source, the shorter the induction time. In the case of addition of 0.375 mL of oil, the induction time is about 15 min. If 3.75 mL is added, the induction time reaches 2 h (Table 2). The second stage is the growth of a dense layer of solid products above the organic phase. This layer consists preferentially of small particles with some very small fibers present among them. The layer reaches a maximum thickness of about 4 mm where it is stable in a third stage before becoming irregular. In the meantime, a solid film appears at the phase boundary. Figure 5a shows the thickness of the layer of solid products as a function of time. It can be seen that the more oil is added, the longer the layer remains stable. In the thickness growth period, the growth velocity seems to be constant. However, since many factors could influence this velocity, this is very difficult to interpret. Nevertheless, extrapolation of the growth curve to a thickness of zero allows to determine the induction time which was found to increase with increasing dilution. Alternatively, the total mass of solid products can be measured. This reveals that the reaction rate of solid formation $r_m = dm/dt$ increases with TEOS concentra-

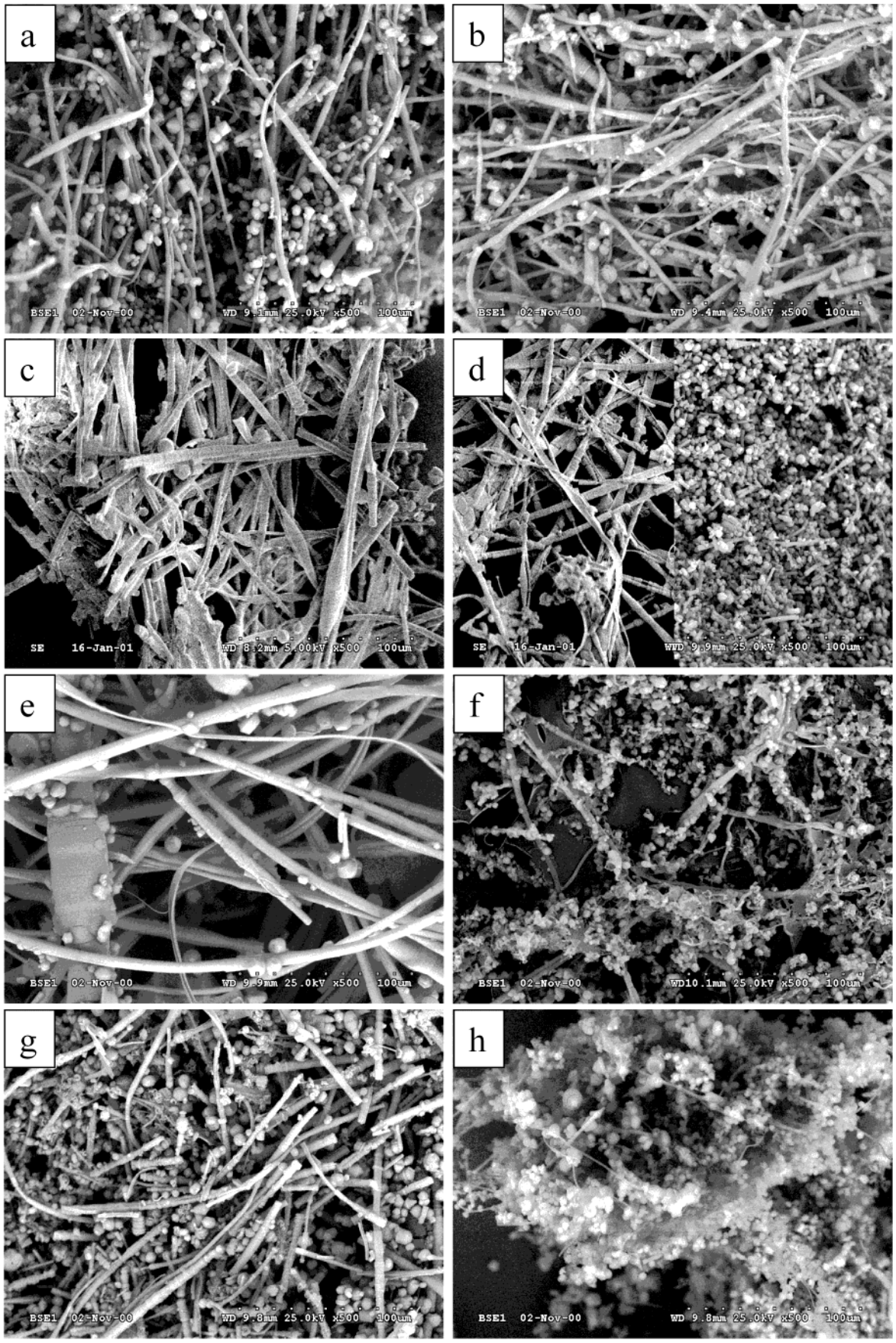

Figure 2. Typical SEM images of synthesis products: (a, b) TEOS in hexane (0.375 mL/3.75 mL); (c, d) TEOS in CCl_4 (0.375 mL/3.75 mL); (e, f) TPOS in hexane (no oil/1.5 mL); (g, h) TPOS in CCl_4 (0.075 mL/1.5 mL). Left pictures: low additional oil volume; right pictures: high oil volume as indicated.

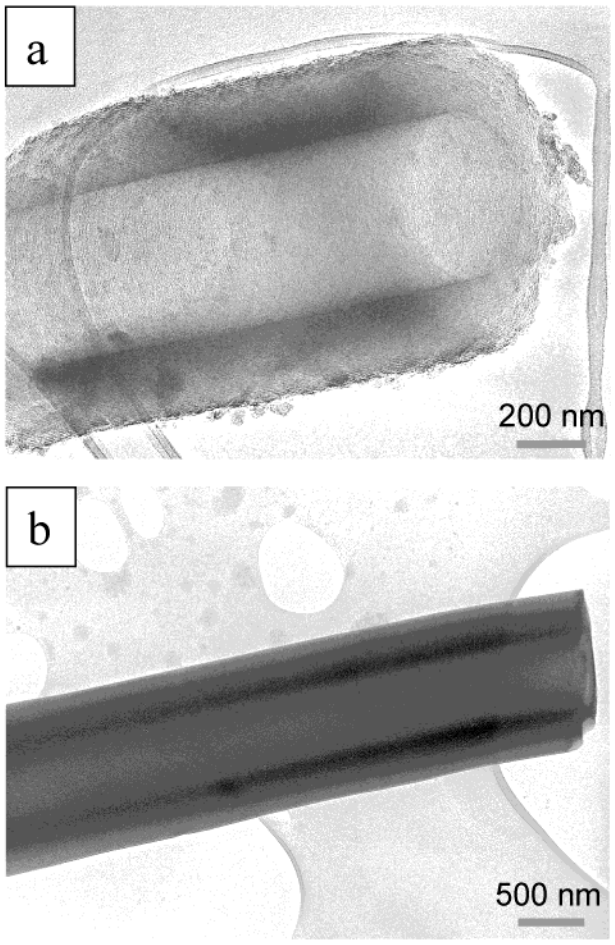

Figure 3. (a) TEM picture of a hollow fiber from TEOS in 1.5 mL of CCl_4. (b) TEM picture of a hollow fiber obtained with TPOS in 0.75 mL of CCl_4.

Table 1. Percentage of Fibers Obtained in the Different Systems[a]

systems	no oil	0.375 mL[b]	0.75 mL[b]	1.5 mL[b]	3.75 mL[b]
TEOS/hexane	52	56	65	65	80
TEOS/CCl_4	76[c]	78	59	54	47
TPOS/hexane	90	90	45	25	
TPOS/CCl_4	65[c]	30	30	10	

[a] The whole synthesis product consists of fibers and small particles. The ratios of both products have been determined from SEM pictures taken after 7 days of synthesis for the TEOS-based systems, after 15 days for the TPOS/hexane systems, and after 6 weeks for TPOS/CCl_4 systems. We estimate the error of the ratio determination to ±10%. [b] Amount of additional oil. [c] Synthesis performed with 0.075 mL of CCl_4.

tion in stage II of the growth process, as can be see in Figure 5b.

The fourth stage of the fiber growth is a period during which the aqueous phase slowly turns turbid, leading to the final stage where visible long fibrous objects appear. The same observations are made when TEOS is mixed with hexane. However, the processes are faster in the TEOS/hexane system and thus more difficult to analyze.

The use of TPOS slows down all processes. Very long homogeneous fibers are also found in this system. When TPOS in hexane is used as silicon reagent, reaction times up to 2 weeks are needed. Addition of CCl_4 slows down the reaction rate even more drastically. In this latter case, the presence of CCl_4 delays the fiber growth

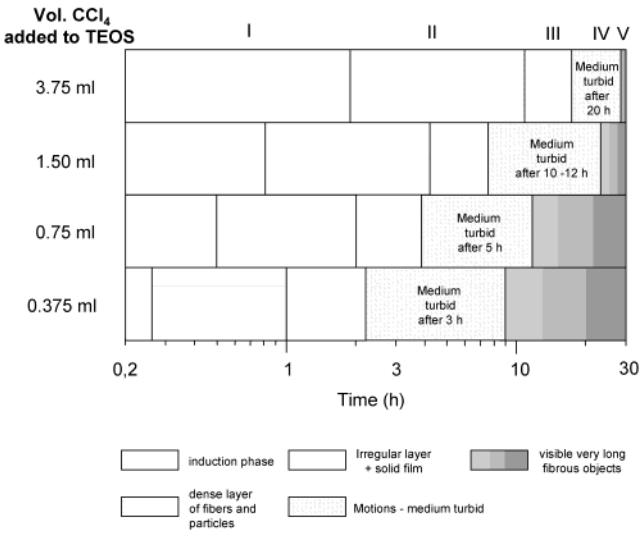

Figure 4. Temporal evolution of a static two-phase acidic system using TEOS in CCl_4 as silica source.

to a time scale ranging from 2 to 4 weeks. However, the same stages in the fibers growth as in the TEOS case are again observed, with very long induction times (several days) and the subsequent presence of a dense layer of solid products during a much longer time (2 weeks).

Internal Structure. The XRD diffraction patterns (Figure 6a−d) show, in all cases, typical hexagonal mesophases with up to four reflections. The intensity ratio of the (110) reflection to the (200) reflection is unusually high in comparison with MCM-41.[1] We assume that this effect is caused by a different wall thickness in comparison with MCM-41.

For the TEOS-based systems (Figure 6a,b), the *d* spacing is not strongly affected by the increasing amount of oil added to the system. The *d*(100) value is observed in the ranges of 4.25−4.3 and 4.26−4.37 nm when hexane and CCl_4 are used, respectively, which is within the experimental error (Figure 7). These values recorded for the TEOS systems are slightly higher than the *d* spacings measured for fibers obtained with TBOS as silicon source (4.1 nm). Furthermore, it should be noted that the structural ordering for products obtained with TEOS in hexane is substantially increased with increasing amount of additional oil. A high-quality hexagonal structure is observed with 3.75 mL of hexane. This fact suggests that longer reaction times lead to more perfectly ordered structures.

The XRD measurements performed on materials obtained from the TPOS-based system show the opposite effect (Figure 6c,d). The well-resolved hexagonal mesophases are observed only at very low oil content. When larger amounts of oil are added to the TPOS reagent, the XRD patterns recorded are different. In the case of hexane addition, the signal-to-noise ratio decreases, suggesting the presence of amorphous products. Also, an increase of the *d* spacing is observed with increasing amount of hexane. The *d*(100) value increases from 4.15 up to 4.4 nm with an oil volume of 1.5 mL (Figure 7). The swelling effect is even more pronounced for the CCl_4 system. Figure 6d shows the XRD diffractograms recorded for fibers from the TPOS/CCl_4 system after 6 weeks of reaction. The hexagonal

Table 2. Growth Kinetics for the System Based on TEOS in CCl_4[a]

systems	induction time t_{ind} (min)	half layer growth time $t_{1/2}$ (min)	v_D (mm/h)	r_m (mg/h)	yield in solution + film (mg/g)
TEOS in 0.375 mL of CCl_4	10 ± 5	25 ± 5	2.3−4.5	2.2	0.10 + 2.15
TEOS in 0.75 mL of CCl_4	30 ± 5	50 ± 5	2.4−4.0	1.5	0.43 + 1.96
TEOS in 1.5 mL of CCl_4	50 ± 5	85 ± 5	2.6 ± 0.4	0.72	0.86 + 1.57
TEOS in 3.75 mL of CCl_4	110 ± 5	160 ± 5	2.4 ± 0.4	0.21	0.74 + 1.40

[a] The phenomenological layer growth velocity v_D was determined via the equation $v_D = 0.5D_{max}/(t_{1/2} - t_{ind})$, where D_{max} is the maximum thickness of the product layer obtained from Figure 5a. The growth rate of the mass of products r_m has been determined from the fitted straight lines in Figure 5b. The yield (mass of products divided by the mass of synthesis solution) was measured after 7 days of synthesis. It has an error of about 0.05 mg/g due to the product removal procedure.

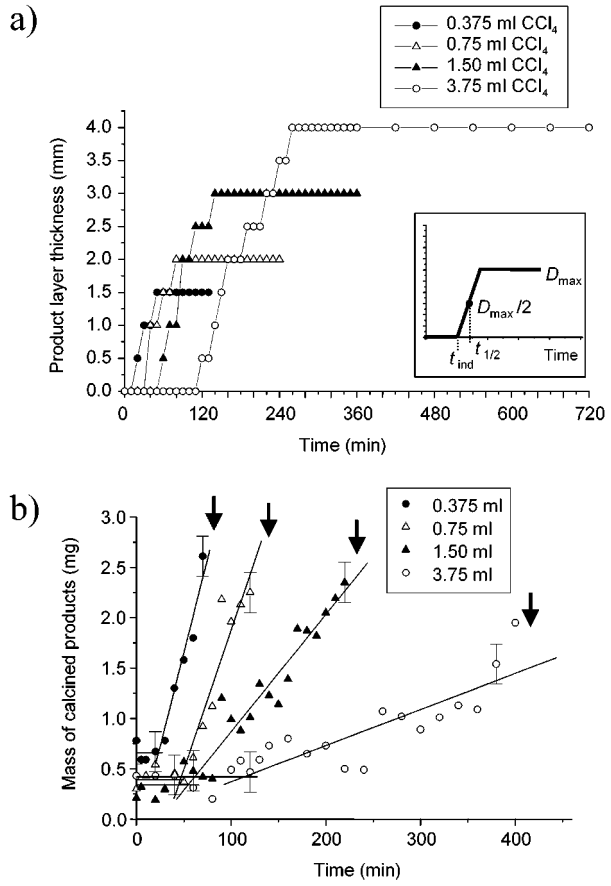

Figure 5. (a) Thickness of the dense layer of solid products observed in stage II and III of the synthesis for the TEOS/CCl_4 systems as a function of time. (b) Mass of solid products obtained after calcination for the same systems as a function of time. The arrow indicates the appearance of the solid film at the interface. Two straight lines were fitted to the data points: a horizontal line averaging the data points before the appearance of visible solid products and a linear rise fitting the data points after the appearance of solid products until the appearance of the solid film disturbing the mass determination.

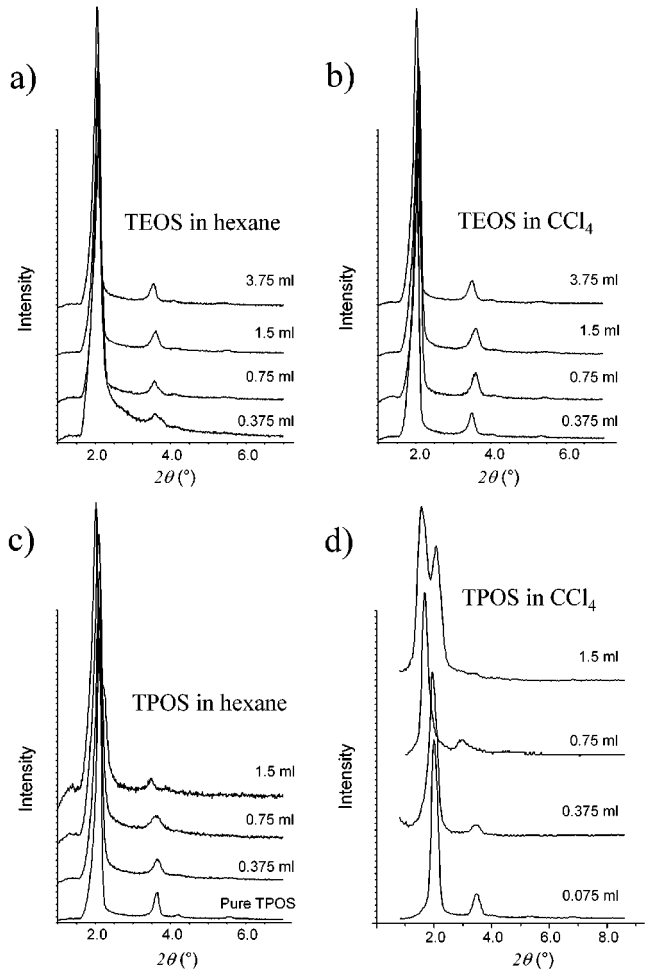

Figure 6. XRD recorded for dried mesostructured fibers: (a) materials obtained from TEOS in hexane, (b) from TEOS in CCl_4, (c) from TPOS in hexane, and (d) from TPOS in CCl_4.

mesophase observed is substantially swollen with CCl_4 and has $d(100)$ values up to 5.15 nm. However, a well-ordered mesophase is formed only at low CCl_4 concentrations. At high CCl_4 volumes (1.5 mL of CCl_4 and higher), the growth of solids is very slow, and the XRD patterns recorded do not show the well-resolved hexagonal phase. No mesostructured fibers have been found among the synthesis products.

The powder XRD measurements show only the local hexagonal pore arrangement, but they cannot reveal the internal architecture of the fibers as micrometer scale objects. TEM investigations give insight into this architecture if a clear correlation exists between the viewing direction in TEM and the macroscopic fiber shape, as was recently demonstrated.[31] Therefore, we correlated our TEM pictures with TEM overview pictures. The TEM pictures (Figure 8) show the presence of a hexagonal array of channels. Since the viewing direction is clearly perpendicular to the fiber axis, as shown in the overview, the channels must be running perpendicularly to the fiber axis. This observation is fully reproducible along the whole fiber. It allows two interpretations: the channels can be closed-off rings or helices. Since the channels can be seen on both edges of the fiber simultaneously (Figure 8d), only a very small pitch angle of a helix is possible, if the structure is helical instead of consisting of closed-off rings.

The circular internal structure is observed for all fibers synthesized in this work. These observations are

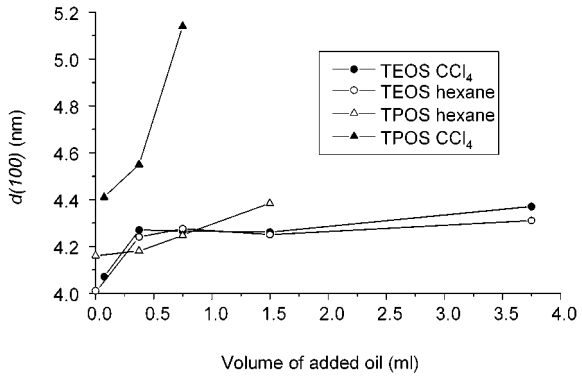

Figure 7. *d*(100) spacing for the different systems investigated as a function of volume of added oil. The *d* spacing of the sample synthesized with pure TBOS is around 4.1 nm.

in agreement with the detailed study of the internal fiber structure for the TBOS system.[31,32]

Additional Modifications. One can also replace hexane and CCl_4 by other additional oils, such as mesitylene or toluene. The addition of these oils to either TEOS or TPOS leads also to mesoporous silica fibers having the same structural properties.

Mesostrutured silica fibers were also synthesized with other surfactants. Fibers were obtained, with TEOS, TPOS, or TBOS as silicon sources, by using the equivalent amount of C14TAB and CTACl. Addition of oils was performed in the same manners as before. The fibers exhibit the same XRD characteristics as those synthesized with CTAB and present the same internal architecture. The use of a shorter chain surfactant leads to materials with smaller *d* spacing values (3.7 nm for the example of fibers based on TBOS) and generally leads to the recovery of a lower amount of solid products (0.9 mg per g of solution for the TBOS-based synthesis). On the other hand, the reaction conducted with CTACl as surfactant and TBOS as silicon source yields a similar amount of solid products as with CTAB (1.75 ± 0.10 mg per g of solution).

Furthermore, in all syntheses described so far the fibers were prepared from a surfactant solution at pH = 0. We have also synthesized mesoporous fibers using the same silicon sources at a higher pH of 0.5. The fibers present the same properties as the ones synthesized at lower pH. No substantial change in the structure and morphology could be observed; however, the growth process is slower, and the yield is slightly lower (1.1 mg per g of solution for the TBOS-based synthesis).

Discussion

Circular Architecture. On the basis of X-ray diffraction and electron microscopy, all the fibers were shown to have a hexagonally ordered mesostructure. The internal architecture of the fibers obtained in strong acidic medium is independent of the silica source: the addition of oil to either TEOS or TPOS does not change the internal ordering of the channels running perpendicular to the fibers axis. One can, therefore, conclude that fibers obtained from TEOS and TPOS with various additional oils have the same internal circular structure observed previously for TBOS as silicon reagent. This fact corrects the former statement of a paper with two of us as coauthors[29] given for fibers from a TEOS-in-oil system, where the channels were described as running parallel to the fibers axis. In this paper the assignment of the TEM pictures to the viewing direction was probably incorrect. Because of the surprising circular architecture which seems to appear generally, former ideas on fiber formation mechanisms have to be reconsidered again.

Despite the identical internal architecture, the different systems described lead to different fractions of the various morphologies. The coexistence of different macroscopic shapes and their very similar internal architecture point to a strongly related formation mechanism.

Possible Formation Mechanism. The processes by which curved shapes and fibers form have attracted much interest.[33−36] It has been recently proposed that the well-defined shapes could be initiated by topological defects[33,34] and that the shape and length of the mesoporous silica products depend strongly on the silica supply and on the self-assembly of the silica and surfactant at the two-phase interface.[37] These suggestions are of a general nature and a good starting point for experiments aimed at a better insight into the nucleation processes on a molecular level, but they are not directed toward an explanation of the circular architecture of the fibers. We therefore proposed a hypothesis for a mechanism that could help to understand the fiber growth processes.[38] We suggested that the basis for the fiber formation is a hypothetical circular seed. The origin of the circular seeds could be explained by the following multistep formation process: (1) formation of a low number of long micelles by a slow aggregation process, (2) spontaneous bending of the rod-shaped micelles leading to loops, and (3) restructuring of the loops to tight coils by lowering of the surface energy. These nanoscopic coils will further grow by addition of new micelles. Finally, elongated circular solids will precipitate in the aqueous phase. As the well-shaped small particles accompanying the fibers have probably a similar internal structure, they are likely formed by a related formation mechanism, where less perfect seeds lead to these shapes instead of fibers.

The formation of hollow fibers has been investigated in a separate paper,[39] showing that the longitudinal growth process of solid fibers can lead to hollow ones. A solid fiber forms a hole in the center during its longitudinal growth if the helical extension process of the fiber center does not proceed completely perfectly. Then, a hollow fiber connected to a solid fiber is formed which are indeed observed among the products.[39]

Swelling Effects. When TEOS or TPOS is used without any additional oil, the lattice parameter is

(33) Yang, H.; Ozin, G. A.; Kresge, C. T. *Adv. Mater.* **1998**, *10*, 883−887.
(34) Sokolov, I.; Yang, H.; Ozin, G. A.; Kresge, C. T. *Adv. Mater.* **1999**, *11*, 636−642.
(35) Yang, S. M.; Sokolov, I.; Coombs, N.; Kresge, C. T.; Ozin, G. A. *Adv. Mater.* **1999**, *11*, 1427−1431.
(36) Lin, H.-P.; Cheng, Y.-R.; Lin, C.-R.; Li, F.-Y.; Chen, C.-L.; Wong, S.-T.; Cheng, S.; Liu, S.-B.; Wan, B.-Z.; Mou, C.-Y.; Tang, C.-Y.; Lin, C. Y. *J. Chin. Chem. Soc.* **1999**, *46*, 495−507.
(37) Yang, S. M.; Yang, H.; Coombs, N.; Sokolov, I.; Kresge C. T.; Ozin, G. A. *Adv. Mater.* **1999**, *11*, 52−55.
(38) Marlow, F.; Kleitz, F. *Microporous Mesoporous Mater.* **2001**, *44−45*, 671−677.
(39) Kleitz, F.; Wilczok, U.; Schüth, F.; Marlow, F. *Phys. Chem. Chem. Phys.* **2001**, *3*, 3486−3489.

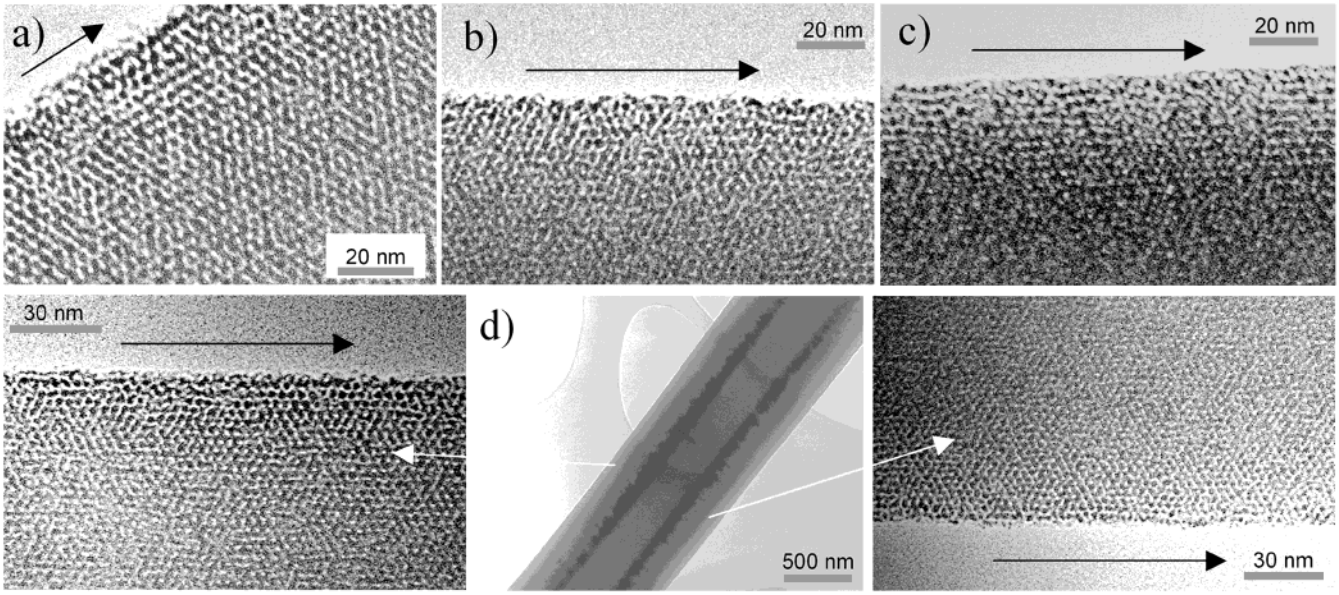

Figure 8. TEM pictures of the edge of mesoporous fiber synthesized with different silica sources: (a) TEOS in CCl_4, (b) TEOS in hexane, (c) TPOS in CCl_4, (d) TPOS in hexane. The hexagonal ordering is visible near the fiber edges for all samples. The arrows indicate the direction of the fiber axis. In the TPOS/hexane case, pictures obtained simultaneously on both sides of a fiber are shown.

comparable to that observed with TBOS, with a *d*(100) spacing of 4.1−4.2 nm. However, the lattice parameters of hexagonal mesophases obtained from TEOS and TPOS in the presence of oil are substantially larger than the lattice parameters measured with fibers from syntheses performed without additional oil. The TEOS-based system is only slightly swollen compared to the pure systems with no significant dependence on the oil concentration. On the other hand, the addition of either hexane or CCl_4 to TPOS leads to a large increase of the *d* spacing values, and a clear dependence on the amount used can be observed.

The influence of oil addition to MCM-41-type materials has already been described in the first publications[1a,b] and has recently been investigated in detail under alkaline conditions.[40] Swelling can be induced even after assembly of the mesophase, as long as the silicate framework is sufficiently flexible due to incomplete condensation. This could be one factor that helps to explain the swelling effects observed in this study: the more hydrophobic and bulky the substituents of the silicon precursor, the slower the hydrolysis rate. Therefore, TEOS forms a rigid framework more rapidly than TPOS and TBOS. The mesophase obtained with TEOS has thus less time to incorporate sufficient amounts of oil to result in a detectable lattice expansion. Since oil is supplied from the interface, it is released slowly to the aqueous phase and thus gradually incorporated in the micelles. Structures formed early, such as the products from the TEOS system, will therefore be swollen to a much lower extent than structures formed after several days.

Morphology. The formation of a high fraction of well-developed fibers seems to require a delicate balance of a sufficiently low rate of hydrolysis and silica condensation and a sufficient flexibility of the micelles to adapt to a homogeneous fiber. Pure TEOS forms silica too rapidly, and the available time is too short for the formation of well-developed homogeneous macroscale structures. Pure TBOS forms the most perfect fibers, and the synthesis time is the longest. The more rapidly reacting silicon sources can be slowed by dilution, but at the expense of oil incorporation (swelling), which makes the initial micelles less flexible. In addition, micelle size will vary over the course of the synthesis due to increasing amounts of oil solubilized in the aqueous phase. Both factors lead to a more error prone assembly of the micelles to larger scale objects, resulting in a higher fraction of small particles. The higher irregularity of the structures formed under such conditions is also apparent in the noisier and less resolved diffraction patterns for the TPOS system with increasing oil concentration. The addition of oil to the different systems has the tendency to inhibit the longitudinal growth of homogeneous fibers and to favor the occurrence of new morphologies among the synthesis products, such as very compressed short fibers, thinner circular units, or hollow solids.

Conclusions

Fibers with the same internal structure have been formed from several different two-phase systems. The fibers are always formed in the aqueous phase, irrespective whether CCl_4, hexane, or other organics are used as the additional oil. This means that the fibers can be formed either above the phase boundary or below. It can therefore be concluded that gravity is not the key factor in controlling fiber growth.

For all fibers collected, the high degree of order is confirmed by transmission electron microscopy, and the hexagonally ordered channels are found to run perpendicularly to the fiber length axis, whirling around the fiber center. This suggests that all the fibers obtained from the two-phase acidic system under static conditions follow the same mechanism of formation.

(40) Lindén, M.; Agren, P.; Karlsson, S.; Bussian, P.; Amenitsch, H. *Langmuir* **2000**, *16*, 5831−5836.

By changing the amount of additional oil and by varying the type of precursors, the ratios of different shapes can be tuned and the kinetics of the fiber growth can be influenced. The fiber growth process can be divided into five experimentally well-separated stages with tunable kinetics, starting with an induction period followed by different growth stages of visible solid products.

Acknowledgment. The authors thank the European Community (project ERB-FMRX CT-96-0084 MESOP and HPRN-CT-99-00025 NUCLEUS) and the DFG (Ma 1745/4-1) for financial support. We are very grateful to H. J. Bongard (SEM) and A. Dreier (TEM) at the electron microscopy department. We also thank Dr. Claudia Weidenthaler for the small-angle XRD measurements and Dr. Mika Lindén (Abo Akademi, Finland) and Dr. Stuart J. Thomson for helpful discussions.

CM0110324